UNDERWATER ACOUSTICS AND SONAR PERFORMANCE IN TURBID ENVIRONMENTS

SD Richards QinetiQ

1 INTRODUCTION

This paper reviews some of the current and recent research carried out by the author and colleagues on the subject of underwater acoustics and sonar performance in undersea environments characterized by relatively high concentrations of suspended inorganic particles. Whilst the concentrations under consideration are high in terms of natural marine suspensions, we are in fact concerned with suspensions which may be regarded as dilute in acoustic terms.

Suspended solid particles may influence acoustic wave propagation in a number of ways: they may increase the volume absorption coefficient of the medium through visco-inertial absorption and thermal absorption; they may scatter the sound waves, resulting in increased attenuation of the forward-propagating wave and increased volume reverberation; and they may lead to changes in the sound speed of the medium. For suspensions in which the density ratio between the solid and liquid phases is around 2 or greater, which will usually be the case for mineral particles suspended in water, the thermal absorption term is very small compared with the visco-inertial absorption term, and we can therefore neglect thermal absorption. Similarly, for practical sonar frequencies and naturally-occurring suspension concentrations, the effect of the particles on the speed of sound may be neglected[1].

2 THEORY

2.1 Spherical particles

The absorption of sound in a suspension of small particles was considered theoretically by Sewell[2] in 1910 and, more recently, by Epstein[3]. Sewell considered the case of small, rigid, spherical particles which are taken to be immobile in that they do not oscillate in the sound field. He was interested in the propagation of sound in fogs and clouds, and the assumption of immobile particles is valid for water droplets in air at audio frequencies. However, in the case of aqueous suspensions at megahertz and sub-megahertz frequencies, the particles do respond to the acoustic field and Sewell's theory breaks down.

Lamb[4] extended Sewell's theory to the case of rigid, incompressible particles that are free to move in the sound field. His approach was to obtain an expression for the velocity potential of the waves scattered by such a particle and to obtain the absorption by finding the average rate at which work is done over a large spherical surface surrounding the particle.

Urick[5] obtained the same result as Lamb by employing the expression for the viscous drag developed by Stokes[6]. Isakovich[7] noted that sound propagation in a suspension can produce temperature gradients at the particle-fluid interface, due to the adiabatic character of acoustic waves and may result in a significant attenuation through thermal diffusion. Epstein and Carhart[8] independently deduced the thermal loss contribution in a detailed theoretical examination of the problem. Their work was primarily aimed at attenuation in aerosols, although the bulk of their analysis may also be applied to dispersions in condensed media.

Allegra and Hawley[9], closely following the work of Epstein and Carhart, have extended the theory to include the case of elastic, heat-conducting, solid spheres suspended in a viscous, heat-conducting fluid, and the resulting formulation, sometimes known as the ECAH model, would appear to be the most complete description of the problem. However, the complexity of the model obscures physical insight into the underlying mechanisms. Furthermore, there are a number of difficulties associated with implementing the ECAH model including: a number of typographic errors in the original papers; very large amplitudes arising in the values of the spherical Bessel and Hankel functions; and a resulting matrix equation which is ill-conditioned. It has been shown[1] that the predictions of Urick's expression for visco-inertial absorption, coupled with a simple, heuristic expression for the attenuation due to scattering[10], are in reasonable agreement with the predictions of the ECAH model over the range of particle sizes likely to be found in suspension in the sea, at practical sonar frequencies. Therefore these simpler models have been used for the basis of the results presented in this paper.

The additional contribution to the plane wave attenuation coefficient due to a suspension of solid particles, neglecting thermal absorption, may be written

$$\alpha_{\mathrm{p}} = \alpha_{\mathrm{v}} + \alpha_{\mathrm{s}}\,, \tag{1}$$

where the subscripts v and s refer to the visco-inertial absorption and scattering contributions respectively.

For dilute suspensions of spherical particles the visco-inertial absorption coefficient is given by[5]

$$\alpha_{\mathrm{v}} = \frac{\phi k(\sigma-1)^2}{2}\left[\frac{s}{s^2+(\sigma+\tau)^2}\right], \tag{2}$$

where ϕ is the volume fraction of suspended particles, k is the acoustic wavenumber, σ is the fluid-solid density ratio, and τ and s are, respectively, the coefficients of the inertial and drag terms in the equation for the force acting on the particles, given by

$$\tau = \frac{1}{2} + \frac{9}{4}\left(\frac{\delta_{\mathrm{v}}}{\mathrm{a}}\right) \tag{3}$$

and

$$s = \frac{9}{4}\left(\frac{\delta_{\mathrm{v}}}{\mathrm{a}}\right)\left(1+\frac{\delta_{\mathrm{v}}}{\mathrm{a}}\right). \tag{4}$$

In these equations a is the particle radius and $\delta_{\mathrm{v}} = \sqrt{2\nu/\omega}$ is the skin depth for shear waves in the fluid, where ν is the kinematic viscosity and ω is the angular frequency of the acoustic waves.

The attenuation due to scattering by suspended particles may be determined using the common high-pass approximation[10]

$$\alpha_{\mathrm{s}} = \frac{\phi K_\alpha x^4}{a\left(\frac{4}{3}K_\alpha x^4 + \xi x^2 + 1\right)}, \tag{5}$$

where $x=ka$ is the dimensionless size parameter, K_α contains the dependence on density and compressibility contrasts[10] and ξ is a free parameter controlling the behaviour of the function for intermediate values of x between the Rayleigh (small x) and geometric (large x) regimes.

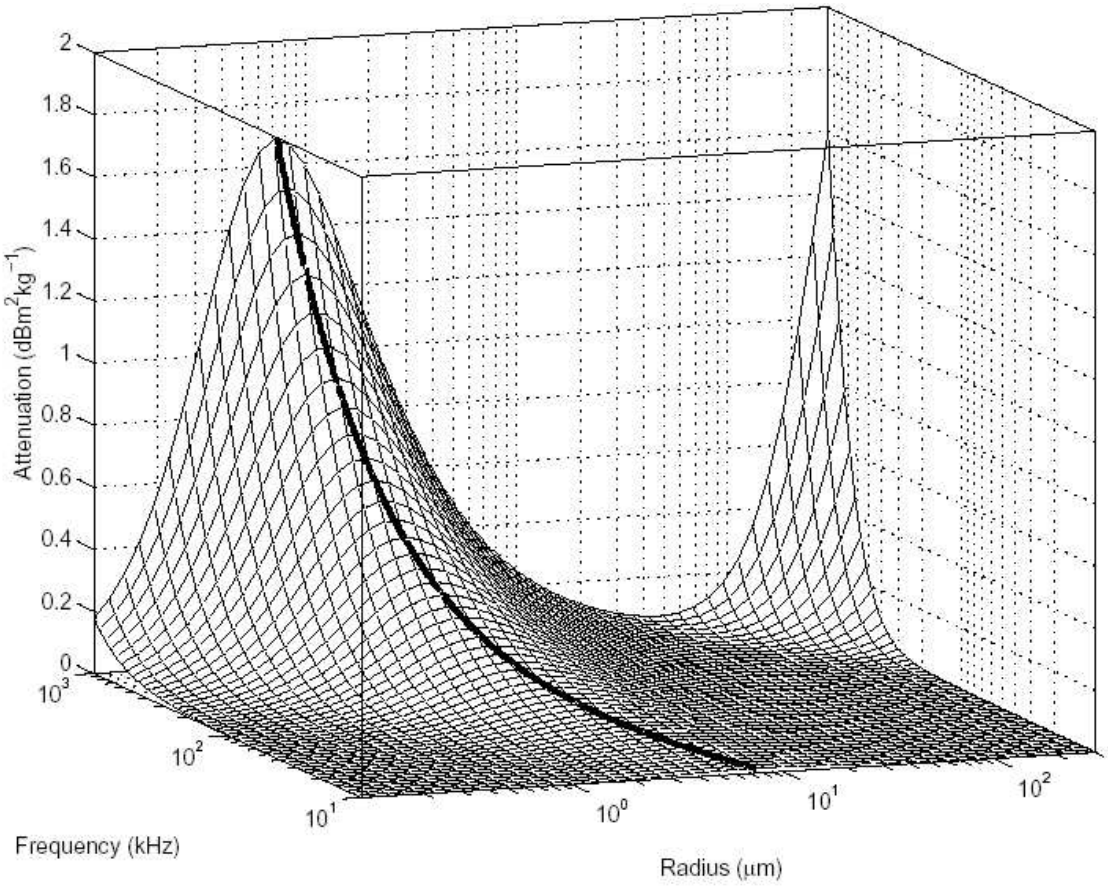

Figure 1: Normalized attenuation as a function of frequency and particle radius, for quartz-like spherical particles suspended in water.

Figure 1 shows the additional attenuation due to a suspension of quartz-like spherical particles in water, as a function of particle radius and acoustic frequency. This figure was calculated using Equations 2 and 5, and the results have been normalized with respect to concentration. The large peak which dominates much of the parameter space is due to the visco-inertial absorption term, whilst the peak at the extreme of high frequency and large particle size is due to scattering in the Rayleigh regime. It will be noted that the peak in the visco-inertial absorption shifts to larger particle sizes as the acoustic frequency is reduced.

2.2 Non-spherical particles

Thus far only spherical particles have been considered. Natural marine particles are not, of course, spherical and an approach is required to estimate the attenuation due to non-spherical particles in suspension. To attempt this by employing scattering theory, such as the ECAH model, involves significant additional complication and the problem rapidly becomes intractable.

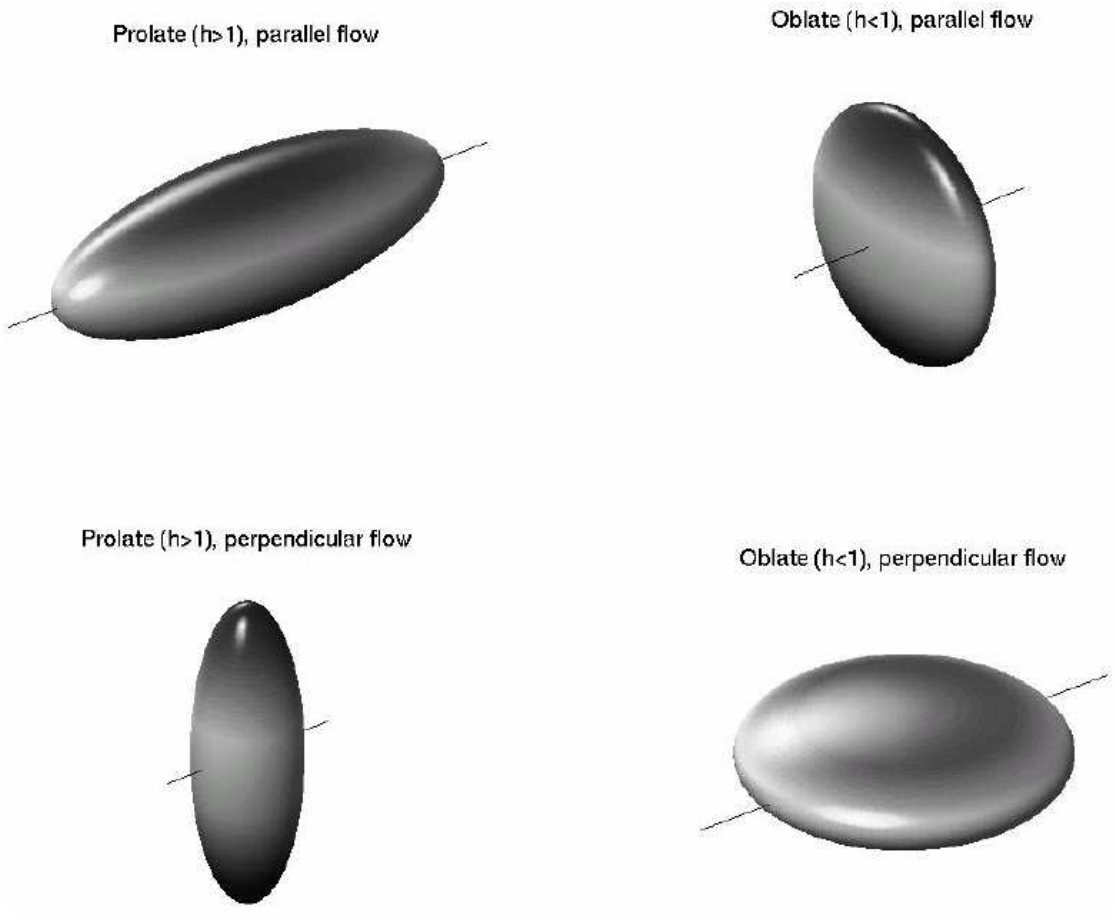

Figure 2: Oblate and prolate spheroids orientated with their axes of symmetry parallel or perpendicular to the direction of motion through the fluid. The motion is parallel to the axis plotted.

Equation 1 may be extended to account for spheroidal particles of the forms shown in Figure 2 by employing suitable expressions for τ and s [11]

$$\tau = L_{\mathrm{i}} + \frac{9}{4}\left(\frac{\delta_{\mathrm{v}}}{b'}\right)K_{\mathrm{sf}}^2 \tag{6}$$

and

$$s = \frac{9}{4}\left(\frac{\delta_{\mathrm{v}}}{b'}\right)K_{\mathrm{sf}}^2\left[1+\left(\frac{1}{K_{\mathrm{sf}}}\right)\left(\frac{\delta_{\mathrm{v}}}{a'}\right)\right], \tag{7}$$

where L_{i} is an inertia factor, K_{sf} is a shape factor and a' and b' are, respectively, the semi-major and semi-minor axes for oblate spheroids and the semi-minor and semi-major axes for prolate spheroids. In the case of spheres $L_{\mathrm{i}} = 1/2$, $K_{\mathrm{sf}} = 1$, $a' = b' = a$ and Equations 6 and 7 reduce to Equations 3 and 4 respectively.

The kaolin particles used in the experiments described in Section 3[12] are plate-like in form, and these particles may therefore be represented as oblate spheroids, the degenerate form of which is a

circular disk. The inertia coefficient for oblate spheroids oscillating parallel to their axis of symmetry is given by[4]

$$L_{\mathrm{ob},\parallel} = \frac{\alpha_0}{2-\alpha_0} \ , \tag{8}$$

where

$$\alpha_0 = \left(\frac{2}{\varepsilon^2}\right)\left[1-\sqrt{1-\varepsilon^2}\left(\frac{\sin^{-1}\varepsilon}{\varepsilon}\right)\right], \tag{9}$$

with the eccentricity ε given by

$$\varepsilon = \sqrt{1-\frac{b'^2}{a'^2}} \ . \tag{10}$$

For oblate spheres oscillating perpendicularly to their axis of symmetry, the inertia coefficient is

$$L_{\mathrm{ob},\perp} = \frac{\gamma_0}{2-\gamma_0}, \tag{11}$$

where

$$\gamma_0 = \frac{\sqrt{1-\varepsilon^2}}{\varepsilon^3}\sin^{-1}\varepsilon - \left[\frac{1-\varepsilon^2}{\varepsilon^2}\right]. \tag{12}$$

The shape factor for oblate spheroids with $h = b'/a' < 1$, for motion parallel to the axis of symmetry, is given by[13]

$$K_{\mathrm{ob},\parallel} = \frac{8}{3}\left\{\frac{2h}{1-h^2} + \frac{2\left(1-2h^2\right)}{\left(1-h^2\right)^{2/3}}\tan^{-1}\left[\frac{\left(1-h^2\right)^{1/2}}{h}\right]\right\}^{-1} \ , \tag{13}$$

and

$$K_{\mathrm{ob},\perp} = \frac{8}{3}\left\{-\frac{h}{1-h^2} - \frac{2h^2-3}{\left(1-h^2\right)^{3/2}}\sin^{-1}\left(1-h^2\right)^{1/2}\right\}^{-1} \ . \tag{14}$$

It has been shown experimentally[14, 15] that scattering from non-spherical particles behaves very much like scattering from spheres when averaged over all particle orientations. Therefore the details of scattering from non-spherical particles are not considered in this paper.

3 EXPERIMENT

3.1 Method

Whilst the ultrasonic attenuation may be significant in the sea over ranges of the order of hundreds of metres, it can be a challenging quantity to measure in a laboratory-scale experiment. This is because the loss per metre is very small, and typically very much smaller than other acoustic losses

in the system, especially the boundary losses. To address this problem a reverberation time method was developed[16], using the apparatus shown schematically in Figure 3a, and photographically in Figure 3b. In this apparatus a test volume of 16 litres of filtered, degassed water is contained within a thin-walled (30 μm) plastic membrane, surrounded by air. This results in a boundary condition which is a good approximation to a pressure-release boundary with a reflection coefficient close to -1, such that boundary losses are minimized.

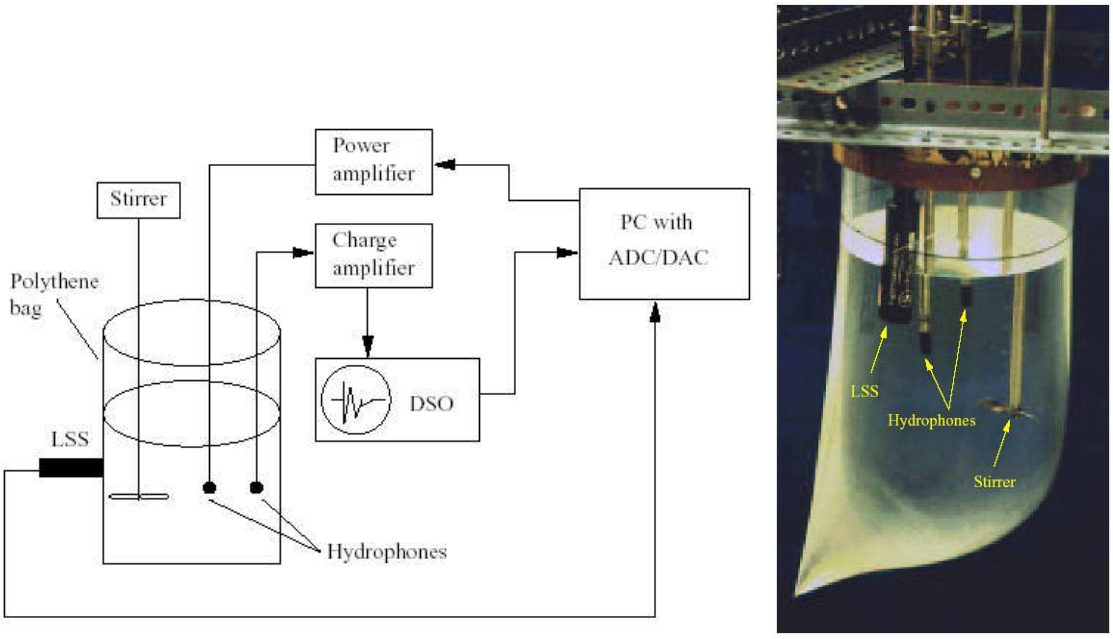

a) b)

Figure 3: a) Schematic of the experimental apparatus for measuring absorption in dilute particulate suspensions. b) Photograph of the apparatus, showing the light scattering sensor (LSS), the two hydrophones, and the stirrer. The diameter of the bag at the water surface was 235 mm. The hydrophones are mounted in rigid tubes to prevent movement. The majority of experiments were carried out with the LSS mounted horizontally on the outside of the bag, and the stirrer was removed during acoustic measurements.

As shown in Figures 3a and b, two hydrophones are present within the water volume, both of which are Brüel and Kjær 8103 hydrophones. One of these is used as a transmitter, exciting the volume into reverberation by transmitting a sequence of 20 ms bursts of pseudo-random noise. The other is used as a receiver, measuring the decay of the reverberant sound field. By measuring the reverberation time of the volume of clear water, t_{60}, then the reverberation time, t'_{60}, in water to which a known quantity of particles have been added, the additional attenuation may be determined from

$$\Delta\alpha = \frac{60}{c}\left(\frac{1}{t'_{60}} - \frac{1}{t_{60}}\right), \tag{15}$$

provided that the addition of the particles does not significantly affect: the sound speed in the medium; the volume of the fluid; the absorption at the boundaries. It has been shown[1] that these conditions were met in the experiments described here.

Also shown in Figure 3 is a light scattering sensor (LSS) which was used to monitor the concentration during experiments, and a mechanical stirrer which was used to resuspend the

particles between experiments. Neither of these items were present in the water during acoustic measurements.

Ideally the reverberation time should be determined from the decay of a diffuse sound field, that is to say one in which the average energy density is the same throughout the entire volume and all directions of propagation are equally probable[17]. The onset of a diffuse field in an enclosure can be described by the Schroeder cut-off frequency[18], which gives an indication of the lowest frequency at which the modal density, i.e. the number of modes per unit bandwidth, is sufficient to constitute a diffuse field. The Schroeder cut-off frequency, f_s, may be written

$$f_s = \left(\frac{c^3}{4\ln 10}\right)^{\frac{1}{2}} \left(\frac{t_{60}}{V}\right)^{\frac{1}{2}}, \tag{16}$$

where c is the speed of sound and V is the volume of the enclosure. The Schroeder cut-off frequency for the volume used in these experiments was typically in the range 50 kHz to 75 kHz, depending on the reverberation time and hence on the absorption in the volume.

3.2 Results

Initial experiments were carried out using a suspension of spherical glass particles, enabling direct comparison with the theoretical predictions for visco-inertial absorption in suspensions of spherical particles. Figure 4 shows some example results for these particles. Measured attenuation data for three different concentrations are plotted against frequency. These data have been processed to yield results at integer multiples of 10 kHz, but the data plotted have been offset slightly in frequency in order that the individual error bars may be resolved. The theoretical curve was obtained by integrating Urick's equation (Equation 2) over the particle size distribution, which was measured by laser diffraction analysis. This figure demonstrates very good agreement between the predictions and measurements for spherical particles.

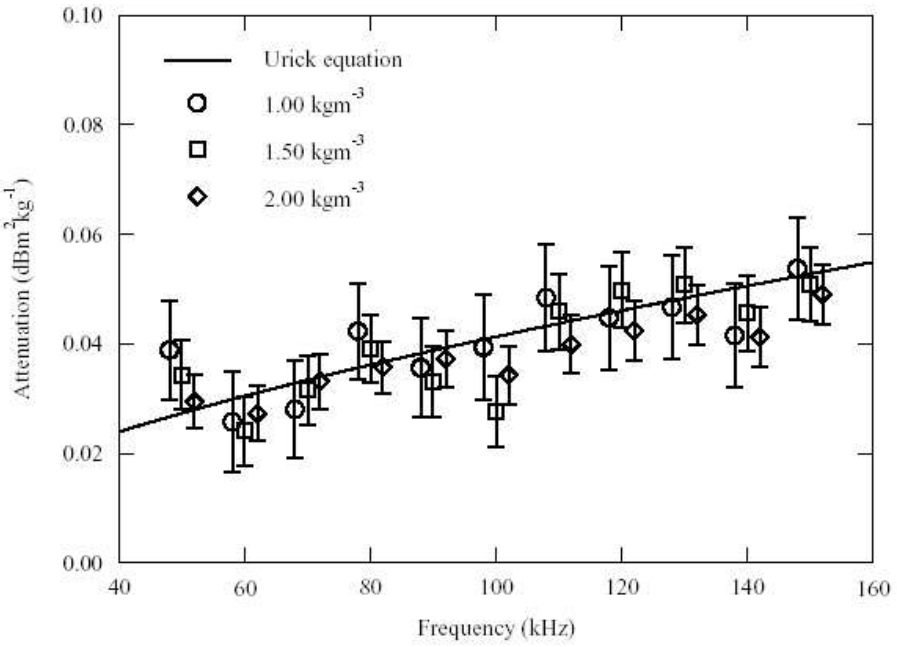

Figure 4: Normalized absorption coefficient for spherical particles: experimental data and prediction using Urick's equation. The data points have been offset in frequency as described in the text.

Of course, natural marine sediment particles are not generally spherical, as shown in Figure 5a, which is a scanning electron microscope image of a sample fine marine sediment particles. This material is difficult to characterize so, as an intermediate step between spherical particles and real sediment particles, measurements have been carried out using well characterized, industrial samples of china clay particles with the trade name 'Speswhite'. These particles are very flat in form, as is shown by the scanning electron microscope image in Figure 5b.

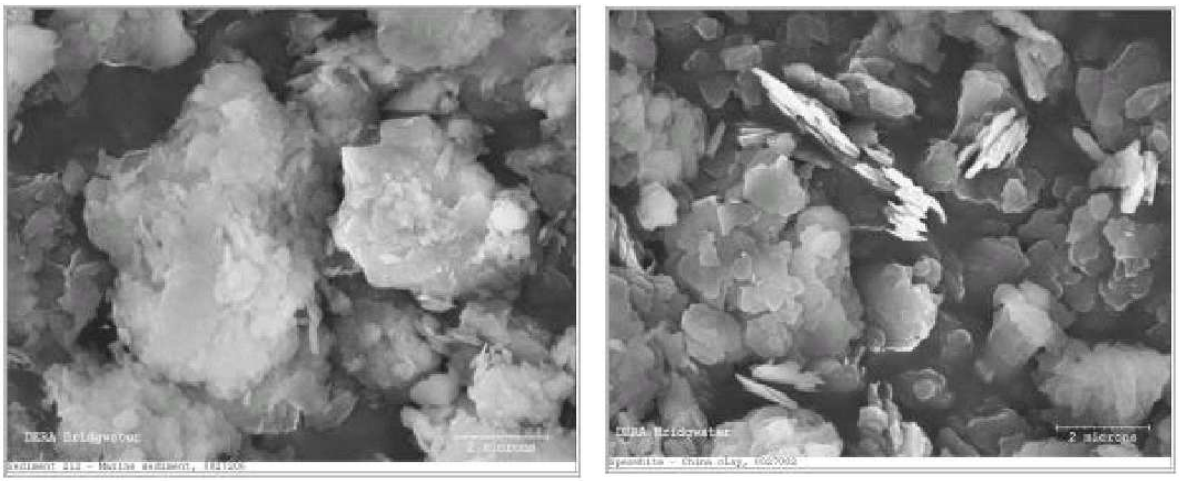

a) b)

Figure 5: Scanning electron microscope images obtained with an original instrument magnification of x10000. a) Natural marine sediment particles, b) 'Speswhite' china clay particles.

The size distribution of the particles was measured by laser diffraction analysis, as was done for the spherical particles, but also by gravitational sedimentation and centrifugal sedimentation. The standard analysis for each of these techniques yields an equivalent spherical diameter, but this will be different for different techniques (an equivalent optical scatter diameter in the case of laser diffraction and a Stokes diameter in the case of the sedimentation methods). The differences between the techniques and the significance of these differences for predicting acoustic absorption in suspensions is discussed elsewhere[19].

In order to predict the absorption due to the Speswhite particles using the spheroidal model it was first necessary to obtain a representative size distribution of spheroids rather than the equivalent Stokes diameters, d_s, yielded by the sedimentation techniques. To achieve this the settling velocity, v_s, was computed for each size bin in the distribution using

$$v_s = \frac{(\sigma - 1) g d_s^2}{18 \nu}, \tag{17}$$

where g is the acceleration due to gravity. From this set of settling velocities the major radii of oblate spheroids with the same set of settling velocities were determined. The Stokes drag force on an oblate spheroid of major radius a' and shape factor K_{sf} settling at velocity v_s in a fluid with molecular viscosity η is given by

$$F_0 = 6\pi\eta K_{sf} a' v_s . \tag{18}$$

Equating this to the gravitational/buoyancy force on the spheroid and rearranging to give a' as a function of v_s yields

$$a'^2 = \frac{18\nu K_{sf} v_s}{4h(\sigma - 1)g}. \quad (19)$$

The aspect ratio for the Speswhite particles is stated by the suppliers to be in the range $\frac{1}{30}$ to $\frac{1}{40}$. It was assumed that the particles were randomly orientated with respect to the acoustic field and, in the absence of shape factors for arbitrary orientation, the calculations were averaged over the two orthogonal orientations, weighted to allow for the one broadside direction and two orthogonal edgewise directions.

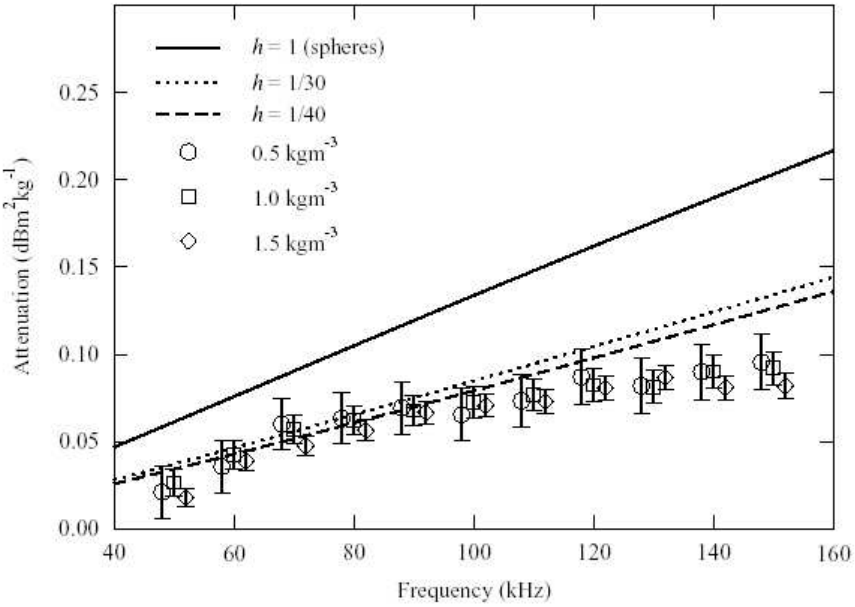

Figure 6: The normalized attenuation coefficient for Speswhite particles: comparison of experimental data with predictions for oblate spheroids. The data points have been offset in frequency as in Figure 4.

Figure 6 shows the measured attenuation in suspensions of Speswhite particles, compared with the predictions of model described in Section 2.2. Calculations are shown for $h = 1$ (spheres), $h = \frac{1}{30}$ and $h = \frac{1}{40}$, corresponding to the aspect ratios quoted by the suppliers. The size distribution of the spheroids was derived from gravitational sedimentation measurements of Stokes diameters using Equations 17 to 19.

This figure shows that the spherical model significantly overestimates the attenuation due to these flat particles, and the predictions based on the nominal aspect ratios of the particles shows significantly better agreement. It is noteworthy that this improved agreement is achieved without assuming any *a priori* information about the measurements when modelling the absorption.

Figure 7 shows the results for the natural marine sediment particles shown in Figure 3a. No aspect ratio data were available for these particles and calculations are shown for $h = 1$, $h = \frac{1}{10}$ and $h = \frac{1}{40}$, spanning the range from spheres to the flattest of the Speswhite particles. It is not apparent whether the spheroidal model yields significantly better agreement with the measurements than the spherical model in this case. Because the sample is characterized by many different particle shapes randomly orientated with respect to the acoustic field, there is an ensemble averaging effect. This means that the spherical particle model gives reasonable agreement with the measurements, even though the individual particles are not spherical.

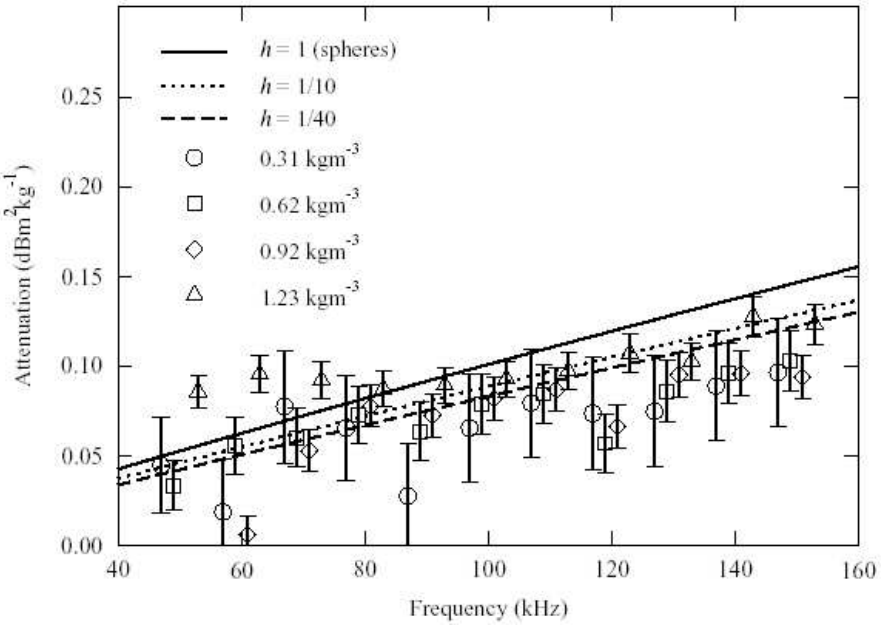

Figure 7: The normalized attenuation coefficient for natural marine sediment particles: comparison of experimental data with predictions for oblate spheroids. The data points have been offset in frequency as in Figure 4.

4 SONAR PERFORMANCE

Sonar performance calculations have been carried out using a ray-based environmental sonar model. This model computes ray paths in a horizontally stratified, range-independent environment assuming a linear sound speed gradient in each horizontal layer. The signal-to-noise ratio along each ray path is calculated using the active sonar equation, including the effects of geometric spreading; volume absorption; surface, bottom and volume reverberation; and various propagating and non-propagating noise contributions.

The additional attenuation due to suspended particles has been incorporated into this model using Equations 1 to 5. The model has further been enhanced[20] by the inclusion of the effects of microbubbles on the volume absorption and the sound speed profile.

Figure 8 shows the computed signal-to-noise ratio for a typical high frequency, shallow water sonar scenario. In this example the water depth was 40 m, the bottom type was mud and the water column was isothermal. The horizontally looking, monostatic projector/receiver was at a depth of 20 m and the source frequency was 80 kHz. The calculations for water containing suspended solid particles assume a monodisperse population of particles with radius 2 μm, density 2600 kg m^{-3}, and a depth-independent concentration of 0.2 kg m^{-3}. A depth-dependent distribution[21] of microbubbles with equilibrium radii in the range 10-200 μm was used, with coefficients chosen to approximate at-sea bubble density measurements[22, 23]. This bubble population is appropriate for the persistent background bubble population in calm, isothermal coastal waters and not for conditions where there is a large surface-generated bubble population.

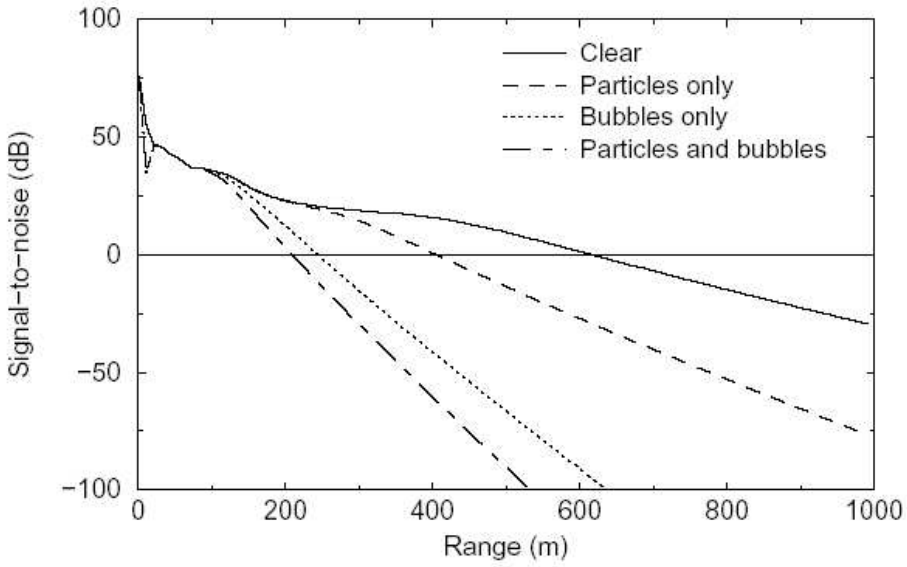

Figure 8: Computed signal-to-noise ratio for a typical high frequency, shallow water sonar scenario (see text) showing the effects of suspended particles and microbubbles.

Taking a 'figure of merit' of 0 dB (shown by the horizontal line in the figure) results in a detection range in clear water of about 615 m in this example. The additional attenuation due to the chosen population of suspended particles reduces this range to 403 m. The bubble population has an even greater effect, reducing the detection range to 243 m, whilst the combined effect of bubbles and suspended particles reduces the detection range to just 209 m.

5 SUMMARY

This papers summarizes some recent and current research by the author and colleagues on the subject of underwater acoustics and sonar performance in turbid environments. Models for visco-inertial absorption by dilute particulate suspensions have been compared with experimental measurements made with suspensions of spherical particles, plate-like clay particles, and natural marine sediment particles. Good agreement was obtained between measurement and prediction for the spherical particles, and the model for absorption by oblate spheroids was shown to give better predictions than the spherical particle model for the refined clay particles. In the case of the marine sediment particles investigated here both models were in reasonable agreement with the measurements, owing to ensemble averaging effects over many different particle shapes.

The effects of both suspended mineral particles and microbubbles on high frequency sonar performance were found to be significant and should therefore be included in high frequency sonar performance prediction models.

6 ACKNOWLEDGEMENTS

The author would like to thank Professor Timothy Leighton and Dr. Niven Brown of the Institute of Sound & Vibration Research, University of Southampton, with whom he collaborated on much of the research described in this paper.

This work was carried out as part of the MoD Corporate Research Programme, and is published with the permission of the Controller of Her Majesty's Stationery Office.

7 REFERENCES

1. S.D. Richards, 'Ultrasonic visco-inertial dissipation in dilute particulate suspensions', *Ph.D. Thesis*, University of Southampton. (2002).
2. C.T.J. Sewell, 'On the extinction of sound in a viscous atmosphere by small obstacles of cylindrical and spherical form', *Phil. Trans. Roy. Soc. London*, **210**, 239-270, (1910).
3. P.S. Epstein, *Contributions to applied mechanics, Theodore von Kármán Anniversary Volume,* California Institute of Technology, (1941).
4. H. Lamb, *Hydrodynamics*, Dover Publications, New York, sixth edition, (1945).
5. R.J. Urick, 'The absorption of sound in suspensions of irregular particles', *J. Acoust. Soc. Am.*, **20**, 283-289, (1948).
6. G.C. Stokes, 'On the effect of the internal friction of fluids on the motion of pendulums', *Trans. Camb. Phil. Soc.*, **IX**, 8-106, (1851).
7. M.A. Isakovich, 'On propagation of sound in emulsions', *Zh. Eksperim. i Teor. Fiz.*, **18**, 907, in Russian, (1948).
8. P.S. Epstein and R.R. Carhart, 'The absorption of sound in suspensions and emulsions I. Water fog in air', *J. Acoust. Soc. Am.*, **25**, 553-565, (1953).
9. J.R. Allegra, and S.A. Hawley, 'Attenuation of sound in suspensions and emulsions', *J. Acoust. Soc. Am.*, **51**, 1545-1564, (1971).
10. J. Sheng and A.E. Hay, 'An examination of the spherical scatterer approximation in aqueous suspensions of sand', *J. Acoust. Soc. Am.*, **83**, 598-610, (1988).
11. A.S. Ahuja and W.R. Hendee, 'Effects of particle shape and orientation on propagation of sound in suspensions', *J. Acoust. Soc. Am.*, **63**, 1074-1080, (1978).
12. S.D. Richards, T.G. Leighton and N.R.Brown, 'Visco-inertial absorption in dilute suspensions of irregular particles', *Proc. R. Soc. Lond. A*, **459**, 2153-2167, (2003).
13. J. Happel and H. Brenner, *Low Reynolds Number Hydrodynamics*, Prentice-Hall, Englewood Cliffs, NJ, 1965.
14. P.A. Chinnery, V.F. Humphrey and J.D. Zhang, 'Low frequency acoustic scattering by a cube: Experimental measurements and theoretical predictions', *J. Acoust. Soc. Am.*, **101**, 2571-2582, (1997).
15. P.D. Thorne, S.B. Sun, J.D. Zhang, I.K. Bjørnø and T. Mazoyer, 'Measurements and analysis of acoustic backscattering by elastic cubes and irregular polyhedra', *J. Acoust. Soc. Am.*, **102**, 2705-2713, (1997).
16. N.R. Brown, T.G. Leighton, S.D. Richards and A.D. Heathershaw, 'Measurement of viscous sound absorption at 50-150 kHz in a model turbid environment', *J. Acoust. Soc. Am.*, **102**, 2705-2713, (1997).
17. L.E. Kinsler, A.R. Frey, A.B. Coppens and J.V. Sanders, *Fundamentals of Acoustics*, Wiley, 3rd Edition, (1982).
18. A.D. Pierce, *Acoustics: an Introduction to its Physical Principles and Applications*, Acoustical Society of America, New York, (1994).
19. S.D. Richards, T.G. Leighton and N.R. Brown, 'Sound absorption by non-spherical particles suspended in water: Comparison of measurements with predictions based on various particle sizing techniques', *Journal of the Acoustical Society of America*, **114**, 1841-1850, (2003).
20. S.D. Richards and T.G. Leighton, 'Acoustic sensor performance in coastal waters: solid suspensions and bubbles', *Acoustical Oceanography*, Eds T.G. Leighton, G.J. Heald, H.D. Griffiths and G. Griffiths, *Proceedings of the Institute of Acoustics*, **23**, Part 2, 399-406, (2001).
21. H. Medwin and C.S. Clay, *Fundamentals of Acoustical Oceanography*, Academic Press, San Diego, (1998).
22. H. Medwin, '*In-situ* measurements of bubble populations in coastal waters', *J. Geophys. Res.*, **75**, 599-611, (1970).
23. H. Medwin, '*In-situ* measurements of microbubbles at sea', *J. Geophys. Res.*, **82**, 971-976, (1977).